nature portfolio

https://doi.org/10.1038/s41586-025-08678-9

Supplementary information

A polyene macrolide targeting phospholipids in the fungal cell membrane

In the format provided by the authors and unedited

Title: A new polyene macrolide targeting phospholipids in the fungal cell membrane

Authors: Qisen Deng[1#], Yinchuan Li[1#], Wenyan He[1], Tao Chen[1], Nan Liu[2], Lingman Ma[2], Zhixia Qiu[3], Zhuo Shang[4]*, and Zongqiang Wang[1]*

1. State Key Laboratory of Natural Medicines, China Pharmaceutical University, Nanjing, Jiangsu 211198, China
2. School of Life Science and Technology, China Pharmaceutical University, Nanjing, Jiangsu, 211198, China
3. Department of Pharmacology, School of Pharmacy, China Pharmaceutical University, Nanjing, Jiangsu, 211100, China
4. School of Pharmaceutical Sciences, Shandong University, Jinan, Shandong 250012, China
[#]These authors contributed equally to this work.

Corresponding Author:
Zongqiang Wang
Contact: State Key Laboratory of Natural Medicines
China Pharmaceutical University
639 Longmian Avenue
Nanjing, Jiangsu 211198, China
Email: zqwang02@cpu.edu.cn

Zhuo Shang
Contact: School of Pharmaceutical Sciences
Shandong University
44 Wenhua West Road
Jinan, Shandong 250012, China
Email: zshang@email.sdu.edu.cn

1. Structure elucidation of mandimycin

Mandimycin was isolated as yellow amorphous powder. HR-ESI-MS analysis returned a protonated molecular ion at *m/z* 1198.6344 $[M+H]^+$ and *m/z* 1196.6228 $[M-H]^-$, indicative of a molecular formula $C_{60}H_{95}NO_{23}$ (Δppm -1.97) requiring 14 double bond equivalents (DBEs). The ultraviolet-visible (UV-vis) spectrum of mandimycin in methanol revealed the wavelengths of maximum absorption at 320, 335, and 352 nm as reported for selvamicin[1], suggesting the presence of a conjugated pentaene moiety. The ^{1}H and ^{13}C NMR spectral data for mandimycin exhibited diagnostic signals for 12 olefinic protons (δ_H 5.60-6.30, δ_C 129.0-136.0), numerous oxygenated methines (δ_C 63.0-87.0), and three carbonyl groups (δ_C 208.4, 174.8 and 170.1), suggesting a highly oxygenated polyene macrolide scaffold for mandimycin. A comprehensive analysis using a range of 2D NMR techniques (i.e., HSQC, HMBC, COSY, TOCSY) facilitated the identification of a 38-membered polyene macrolide scaffold that showcases a distinctive C20-pentaene and C-32 monoene pattern, as depicted in Fig C. This pattern distinguishes it from other documented 38-membered polyene antibiotics like nystatin (C-20 tetraene and C-30 diene), amphotericin A (C-20 tetraene and C-30 diene), candicidin (C-20 heptaene), and amphotericin B (C-20 heptaene). Furthermore, it was confirmed that C-5 is substituted with a ketone group, as supported by the HMBC correlations observed from H-3 (δ_H 4.29), H-4 (δ_H 2.53; 2.59) and H-6 (δ_H 2.42, 2.47) to C-5 (δ_C 208.4).

Given the significance of sugar substitution in the antifungal activity of macrolide polyene antibiotics, our subsequent investigation focused on the sugar components within the structure of mandimycin. Notably, the presence of three sugar moieties in the mandimycin structure was affirmed by the diagnostic signals corresponding to three anomeric carbons ($\delta_{H\text{-}1'}$ 4.49, $\delta_{C\text{-}1'}$ 96.8; $\delta_{H\text{-}1''}$ 4.42, $\delta_{C\text{-}1''}$ 99.5; $\delta_{H\text{-}1'''}$ 4.61, $\delta_{C\text{-}1'''}$ 100.0). Subsequent analysis of COSY and HMBC spectra successfully revealed the presence of an aminosugar mycosamine, a digitoxose, and a 3-*O*-methyldigitoxose. Mycosamine was linked to C-19 of the macrolide, as indicated by the HMBC correlations observed from H-1′ (δ_H 4.49) to C-19 (δ_C 74.7), while digitoxose is connected to C-35, as supported by the HMBC correlation from H-1″ (δ_H 4.42) and C-35 (δ_C 84.1). Additionally, the 3-*O*-methyldigitoxose was found to form a glycosidic bond with digitoxose, specifically between C-1‴ and C-4″, as confirmed by the HMBC correlation from H-1‴ (δ_H 4.61) to C-4″ (δ_C 86.8). NMR data were analyzed using MestReNova 14.2.1.

The stereochemistry of mandimycin was deduced through the combination of ketoreductase (KR) domain sequence alignment, sugar biosynthetic cascade analysis, and NMR comparison with the structures of reported polyene macrolide antibiotics[1-3]. The alignment of KR domain sequences from each mandimycin biosynthetic module revealed that KR2, KR10, KR13, KR14, KR16, and KR18 contain a conserved A-type KR pattern (i.e., SxxxxWxxxxQ/H motif), which is deduced to produce a D-type hydroxyl group. In contrast, KR11 and KR12 encode a conserved B-type KR pattern (i.e., LDD motif), which is proposed to generate a L-type hydroxyl group.

Within the biosynthetic gene cluster of mandimycin, we identified the *mandC*/*mandJ* gene cascade, which is homologous to AmpDIII/AmpDII responsible for mycosamine biosynthesis. Moreover, we identified the *mandO*/*mandP*/*mandU*/*mandS*/*mandR* gene cascade, analogous to the *selSIII*/*selSIV*/*selSVII*/*selSII*/*selSI* gene cascade in the selvamicin biosynthetic gene cluster, known for methyldigitoxose biosynthesis. Hence, it can be inferred that mycosamine and methyldigitoxose are present in the structure of mandimycin. Drawing from the aforementioned evidence, mandimycin is a new polyene macrolide antibiotic featuring unique C-20 pentaene and C-32 monoene patterns, C-35 disaccharide substitution, and C-5 ketone substitution. The absolute configuration of the macrolide skeleton in mandimycin was tentatively assigned as 2*R*, 10*R*, 11*S*, 12*S*, 13*R*, 14*R*, 16*R*, and 18*R* based on megasynthase domain analysis and NMR comparison.

2. Structure elucidation of mandimycin B

Mandimycin B was isolated as brown amorphous powder. HR-ESI-MS analysis returned a protonated molecular ion at *m/z* 924.4957 $[M+H]^+$ and *m/z* 922.4792 $[M-H]^-$, indicative of a molecular formula $C_{47}H_{73}NO_{17}$. The maximum UV-vis absorption of mandimycin B (319, 334, and 352 nm) in methanol aligns with that of mandimycin, indicating the retention of the conjugated pentaene moiety. Comparison of 1D and 2D NMR data for mandimycin B with those for mandimycin revealed the major difference being the absence of resonances for digitoxose and 3-*O*-methyldigitoxose, which is consistent with the fact that mandimycin B is produced from the glycosyltransferase gene knockout strain *S. netropsis* Δ*mandQ*. This conclusion was further validated by the significant upfield shift of C-35 ($\Delta\delta_C$ -7.3) and C-37 ($\Delta\delta_C$ -5.6). Moreover, comparison of the ^1H and ^{13}C NMR data of the mycosamine moiety in both mandimycin and mandimycin B revealed nearly identical chemical shifts, indicating the retention of the mycosamine moiety in mandimycin B. Thus, mandimycin B was identified as the C-35 de-sugar analogue of mandimycin.

3. Hemolytic assay

The hemolytic potential of mandimycin was evaluated in liquid blood solutions according to the method previously reported[4]. Briefly, fresh sterile defibrated sheep blood was centrifuged at 3,000 rpm for 10 min at 4 °C to separate the precipitated blood cells, which were subsequently resuspended in a PBS solution (pH 7.4) at a concentration of 1×10^9 cells/mL. Serial dilutions of the test compounds, with the concentrations ranging from 0.39 μM to 100 μM, were prepared and mixed with the blood cells, resulting in a final volume of 500 μL. 0.5% DMSO and 1% Triton X100 was used as the negative (0% hemolysis) and positive (100% hemolysis) controls, respectively. Following a 3-hour incubation period at 37 °C, the supernatant was collected by centrifugation at 3,000 rpm for 20 minutes and transferred to a 96-well polypropylene plate. The degree of hemolysis is determined by measuring the absorbance of the supernatant at OD_{540} using an enzyme-linked immunosorbent assay (ELISA) reader.

4. Time-dependent killing assay

An overnight culture of *C. albicans* BNCC 186382 was prepared by inoculating a single colony in YPD medium and incubating at 30 °C with shaking at 220 rpm. The saturated culture was then diluted to a final centration of 1×10^6 CFU/mL. Subsequently, 4 mL of the diluted culture was then exposed to various concentrations of mandimycin ranging from 0.5 μg/mL to 8 μg/mL. Control tubes without antifungal agents were prepared in parallel. After 24 hours of incubation, colony counts were determined by plating 100 μL of culture onto YDP agar plates at time intervals of 0, 2, 4, 6, 8, 24, and 48 hours. This experiment was performed in three biological replicates (n=3).

5. Scanning electron microscopy

C. albicans BNCC 186382 culture at various time points during the time-dependent killing assay was subjected to scanning electron microscopy (SEM). Fungal cultures (1 mL) treated with mandimycin were harvested and immersed in 0.1 M phosphate buffer (pH 7.0) for 15-30 min. Cells were fixed with 6% glutaraldehyde at 4 °C for 2 hours and washed three times with 0.1 M phosphate buffer for 15 minutes each. This fixation procedure was repeated three times, followed by additional fixation with 1% osmium tetroxide solution for 1-2 hours. After three rounds of rinses with buffer, cells were dehydrated in graded concentrations of ethanol (30%, 50%, 70%, 80%, 90%, and 95%) for 15 minutes each, followed by two immersions in 100% ethanol for 20 minutes each. The samples were treated with a mixture of ethanol and isoamyl acetate (*v/v* = 1:1) for 30 minutes, followed by treatment with pure isoamyl acetate for 1 hour. Subsequently, they were further dried in a critical point dryer. The samples were coated using a gold-sprayed Hitachi MC1000 and imaging was carried out at 3.0 kV in a HITACHI su8010.

6. Potassium ion release assay

The release of potassium ion was monitored using an OrionSensorLinkPCM-700 pH/ISE meter. A single colony of *C. albicans* BNCC 186382 was cultured overnight in 50 mL of YPD medium at 30 °C. The culture was washed three times with cold assay buffer (pH 7.4, 10 mM Tris-acetate, 100 mM NaCl) to remove medium components and adjust to an OD_{600} of 1.0. The concentration of extracellular potassium ions was monitored at 5-second intervals using pH/ISE meter. At the 180-seconds time point, mandimycin at various concentration (10×MIC, 4×MIC, and 1×MIC) was added and the measurement was continued for an additional 1200 seconds. Data were plotted using GraphPad Prism 9. The assay was performed in three biological replicates..

7. *In vivo* ergosterol extraction and quantification assay

To investigate the ability of mandimycin to extract ergosterol from fungal cell membrane, ergosterol extraction experiment from *C. albicans* BNCC 186382 was

carried out by following the established protocols outlined in a previous study[5]. Amphotericin B and DMSO served as positive and negative controls, respectively. Ergosterol quantification was performed using high-performance liquid chromatography (HPLC), following a previously established method with slight modifications[6]. Briefly, the hexane extracts were re-dissolved in 100 µL methanol and centrifuged at 15,000 g for 10 min to remove any insoluble particles. Each sample (10 µL) was analyzed on an Agilent 1260 Infinity II analytical HPLC system (Poroshell 120 EC C18 column, 2.7 µm, 100 Å, 150 × 3.0 mm, 0.7 mL/min isocratic elution at 70% acetonitrile/methanol with 0.1% trifluoroacetic acid over 15 min; UV-vis detector 280 nm, column temperature 30 °C). Ergosterol standard was also analyzed under the same condition. The experiment was performed in three biological replicates.

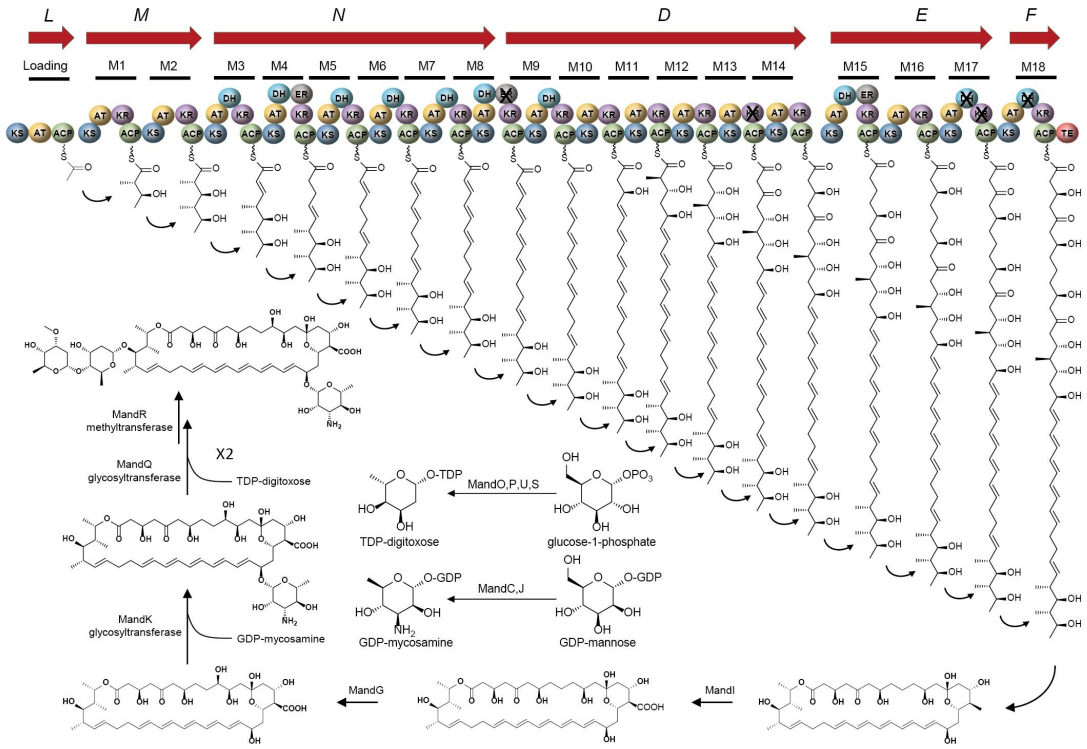

Fig S1. Proposed biosynthetic pathway of mandimycin

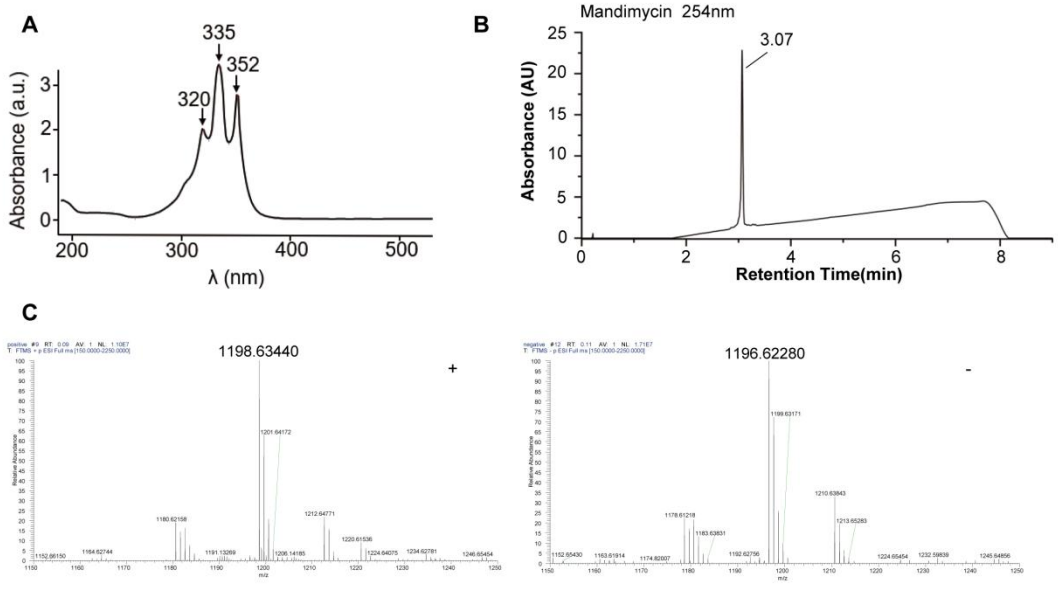

Fig S2. Spectroscopic parameters of mandimycin. (A) UV-vis spectrum of mandimycin showing the wavelengths of maximum absorbance. (B) HPLC spectrum of purified mandimycin detected at the wavelength of 254 nm. (C) HR-ESI-MS spectra of mandimycin under both positive and negative ionization modes.

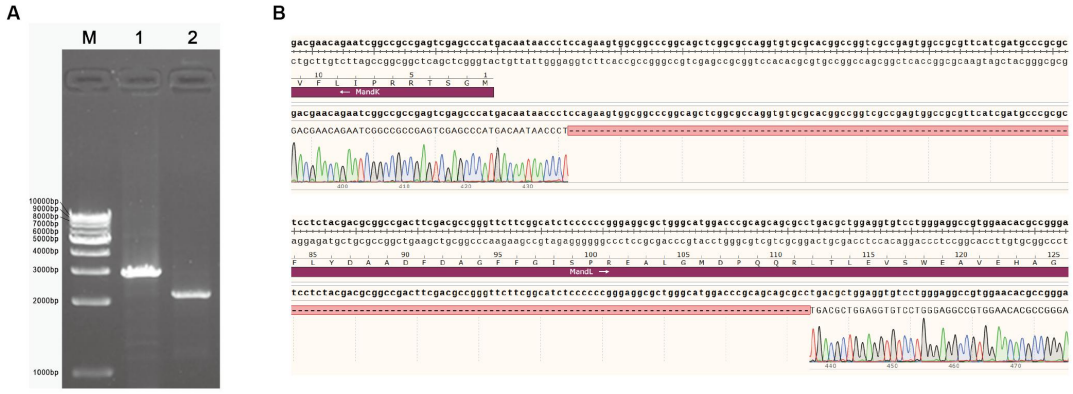

Fig S3. Genetic knockout of a 692 bp fragment in *mandL* within mandimycin gene cluster. (A) PCR amplification of the knockout region in *mandL*. M, 1kb ladder DNA Marker; Lane 1: wide-type (WT) strain; Lane 2: Δ*mandL* mutant; (B) Sanger sequencing confirmed the deletion of 692bp region in Δ*manL* mutant. For gel source data, see SI Figure 1.

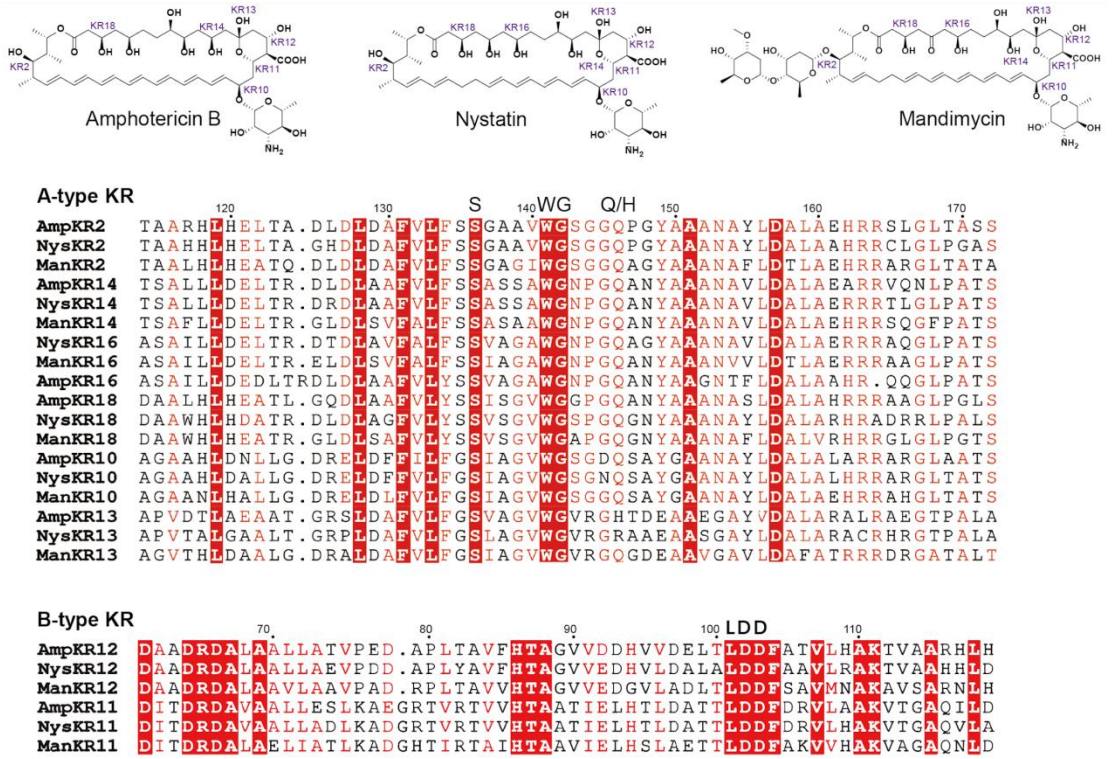

Fig S4. Stereochemistry prediction of mandimycin by alignment of the ketoreductase (KR) domain of amphotericin B, nystatin and mandimycin. A-type KR domains are characterized by a conserved SxxxxWxxxxQ/H sequence, typically associated with the production of D-type hydroxyl (OH) groups. In contrast, B-type KR domain features a conserved LDD motif, which correlates with the biosynthesis of L-type hydroxyl groups. Within mandimycin, KR domains 2, 10, 13, 14, 16, and 18 are classified as A-type, which is responsible for the formation of L-OH, whereas KR domains 11 and 12 are identified as B-type, leading to the generation of D-OH.

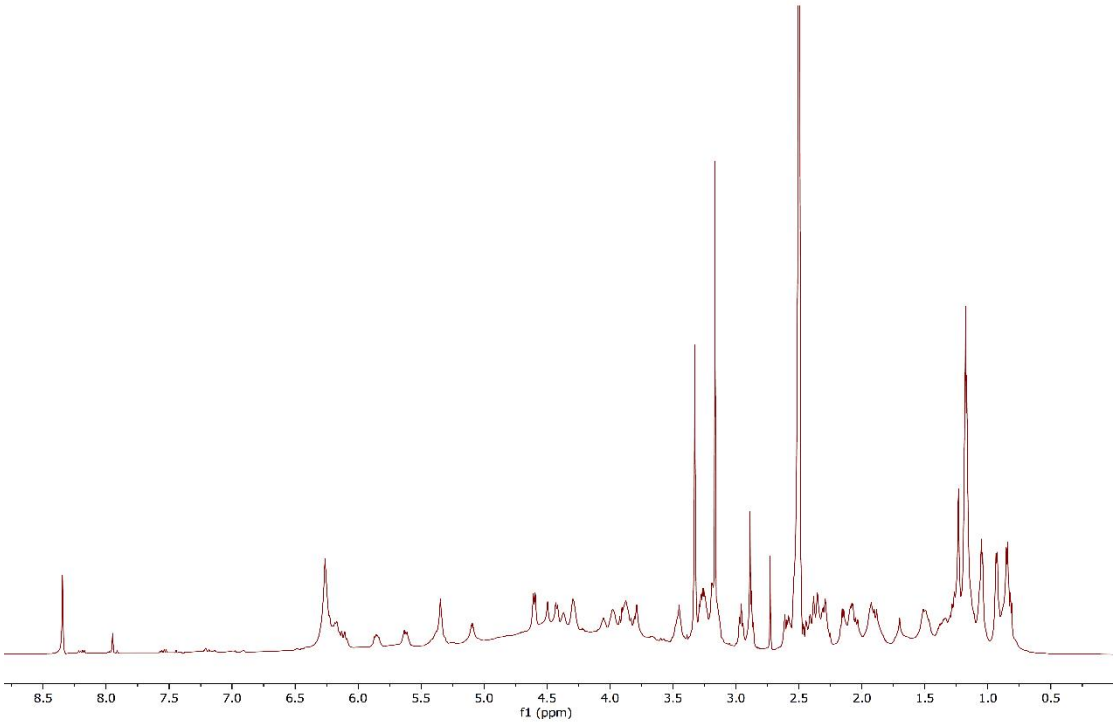

Fig S5. ^{1}H NMR (600 MHz) spectrum of mandimycin in DMSO-d_6

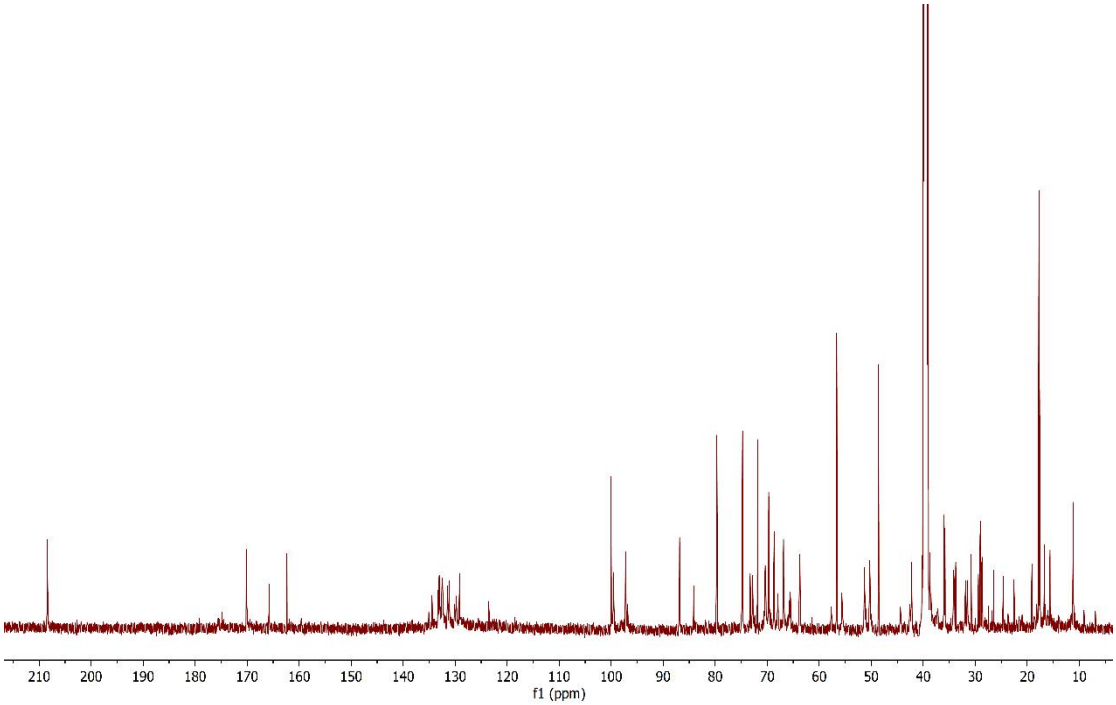

Fig S6. ^{13}C NMR (150 MHz) spectrum of mandimycin in DMSO-d_6

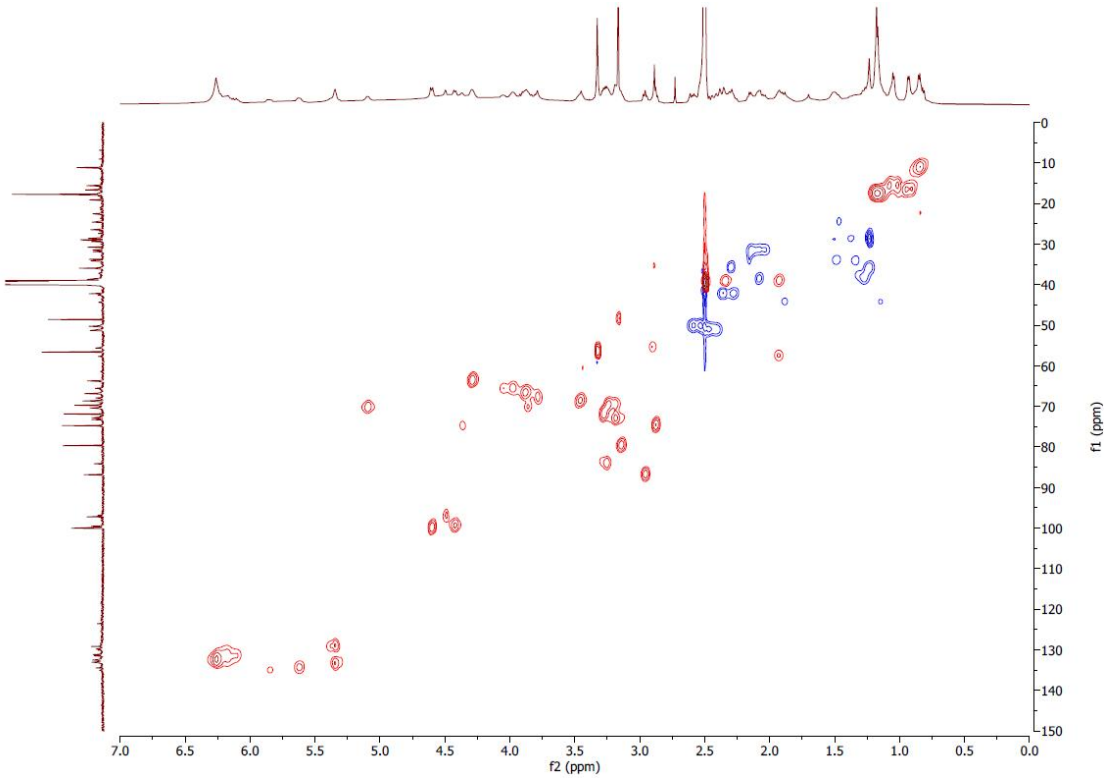

Fig S7. HSQC NMR (150 MHz) spectrum of mandimycin in DMSO-d_6

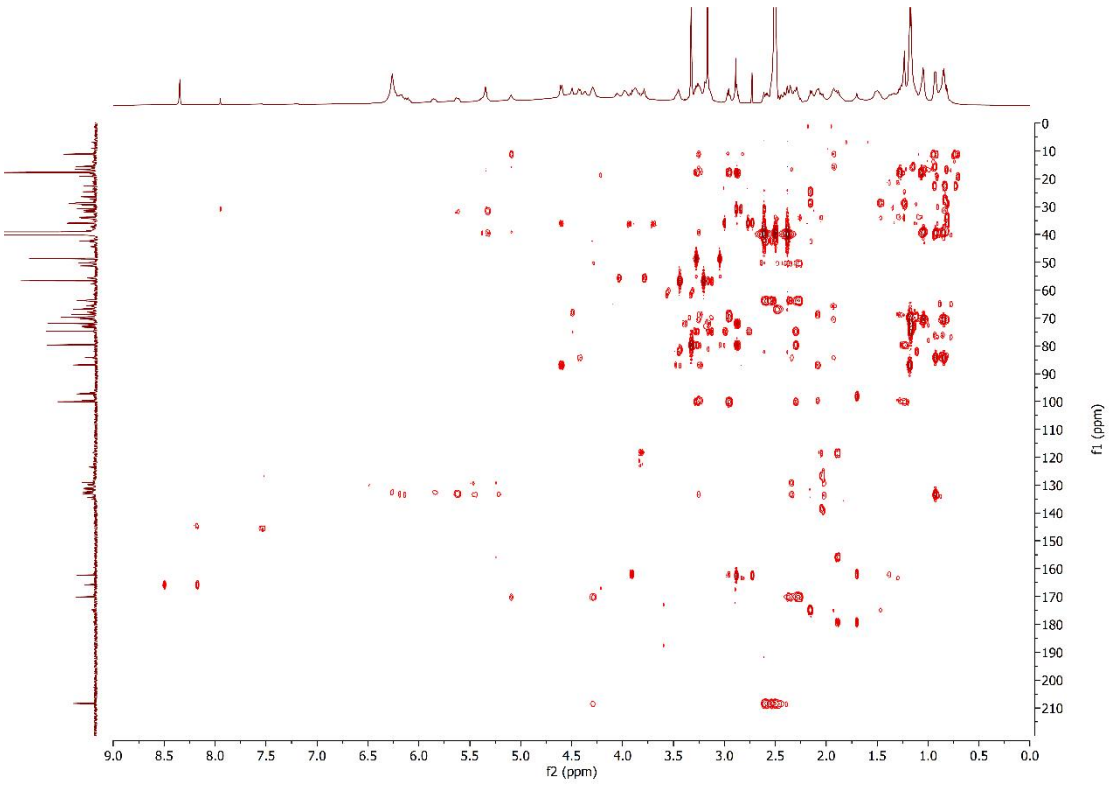

Fig S8. HMBC NMR (150 MHz) spectrum of mandimycin in DMSO-d_6

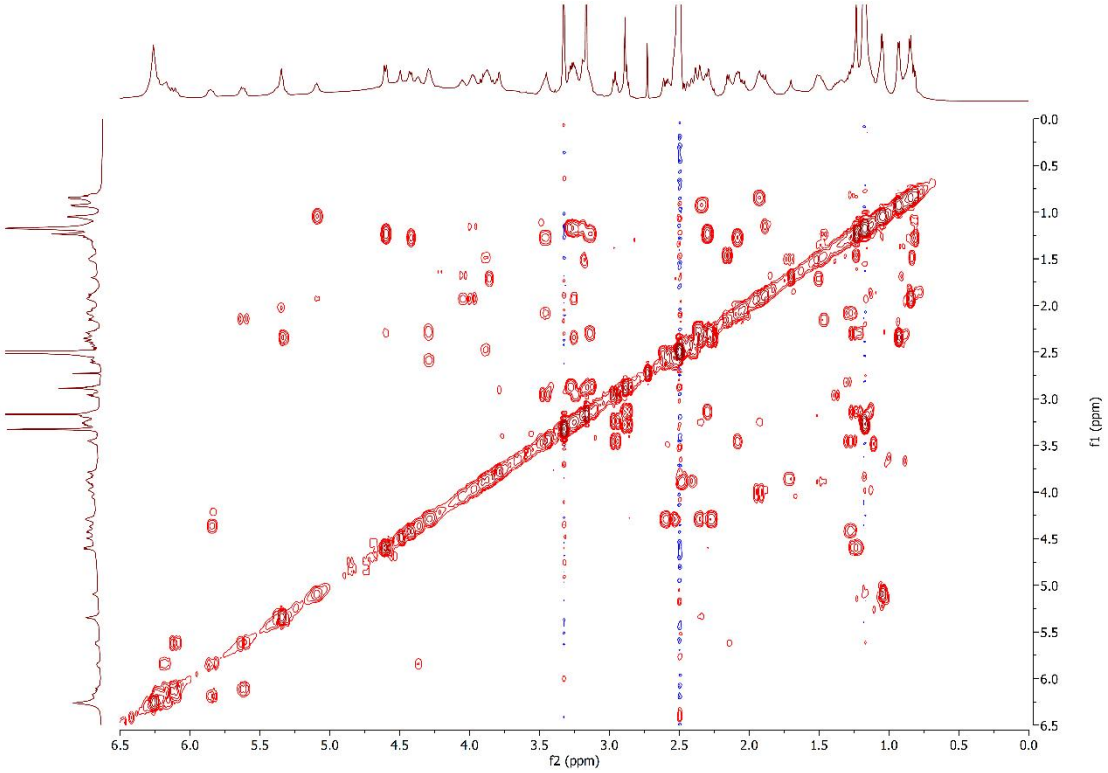

Fig S9. COSY NMR (600 MHz) spectrum of mandimycin in DMSO-d_6

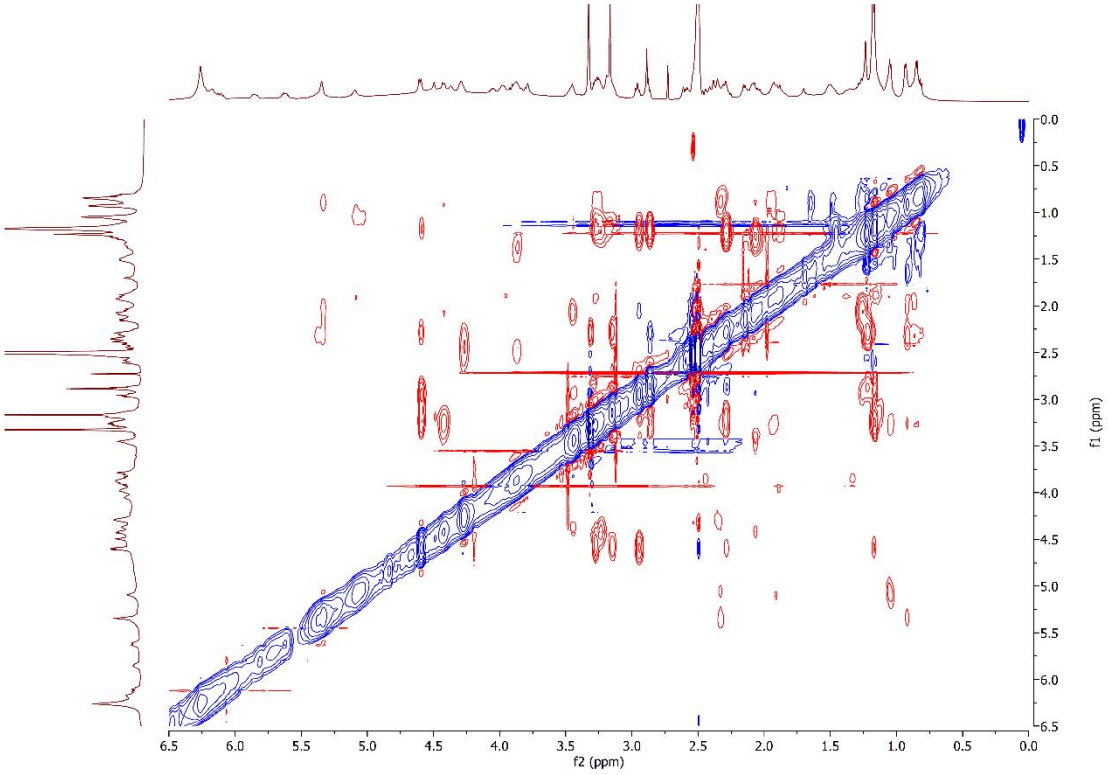

Fig S10. ROESY NMR (600 MHz) spectrum of mandimycin in DMSO-d_6

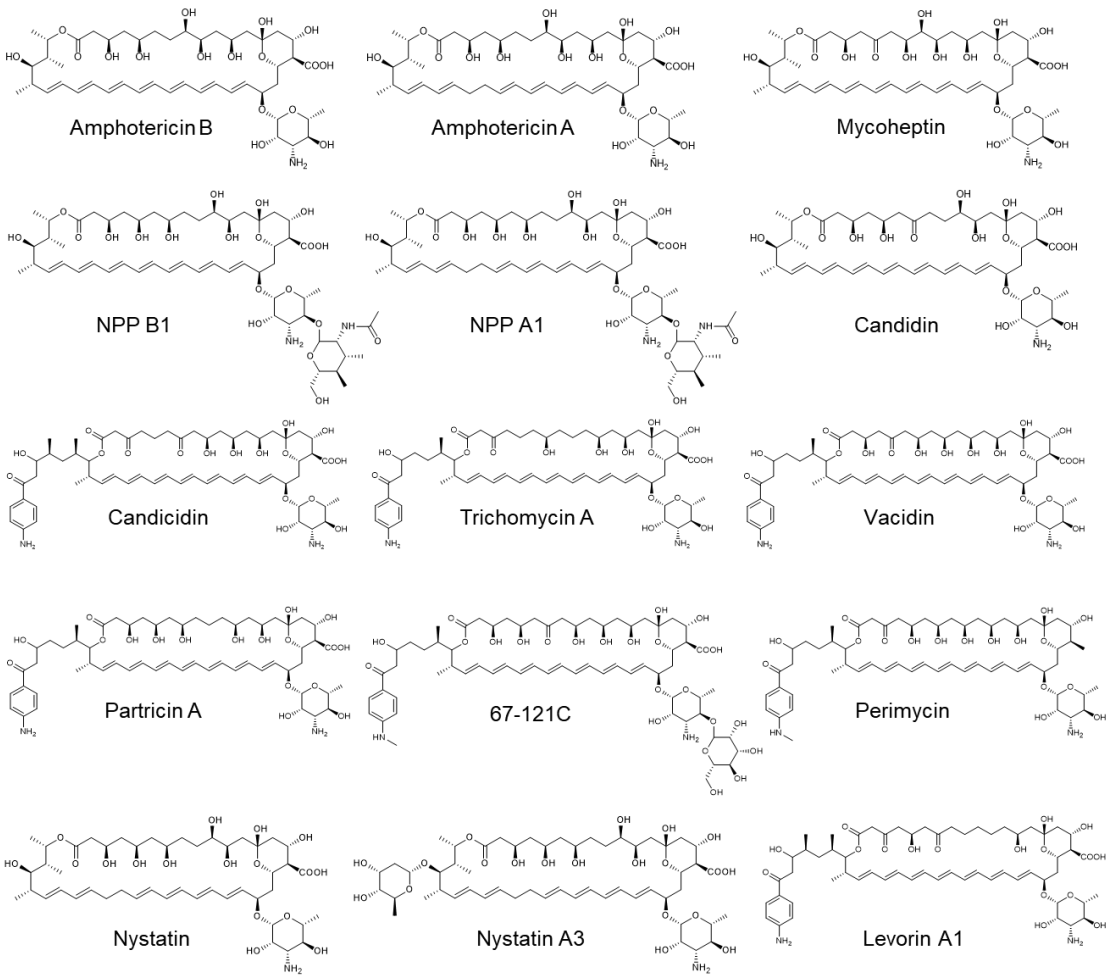

Fig S11. Structures of known 38-membered polyene macrolide antibiotics

A

	Mandimycin	Amphotericin B	Fold(Man/Amp)
Solubility (10 mM TriS-HCl, pH7.4)	8.07 (mg/mL)	0.83 (μg/mL)	9700

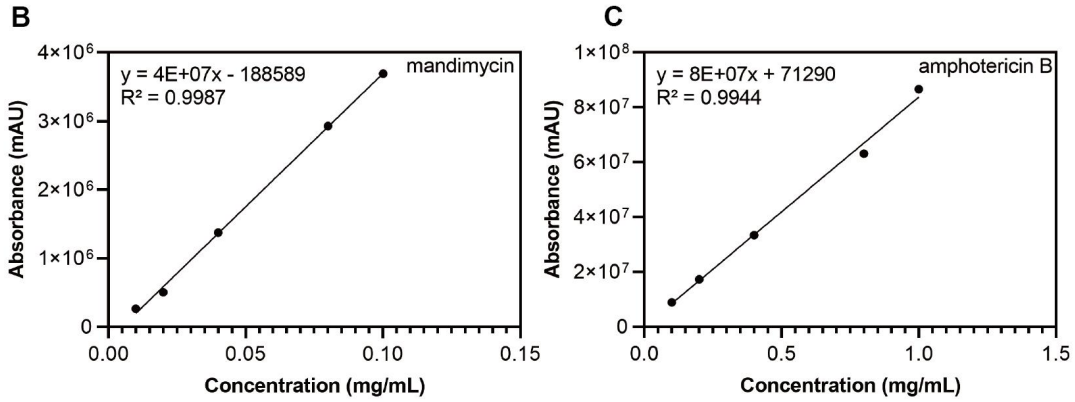

Fig S12. Solubility of mandimycin; (A) Solubility measurement of mandimycin and amphotericin B; (B, C) Standard curve of the amount of solubilized mandimycin and amphotericin B in DMSO and the maximum absorbance values (mandimycin, 334 nm; amphotericin B, 384 nm).

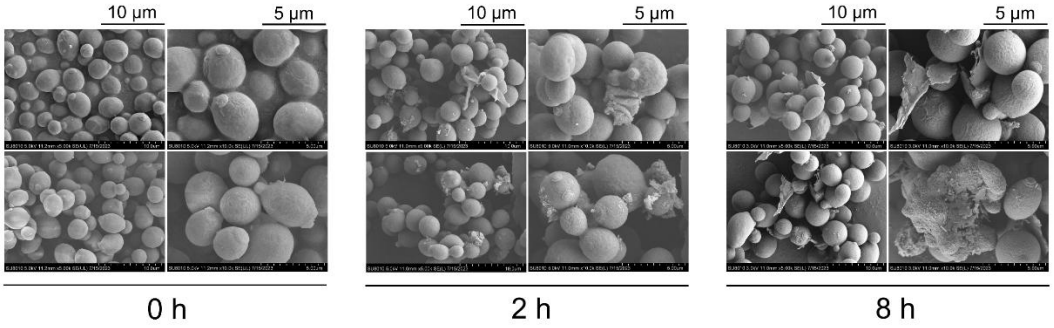

Fig S13. Scanning electron microscopy image of *C. albicans* BNCC 186382 after treatment with mandimycin at 32×MIC concentration. Samples were collected at 0, 2, and 8 hours based on the time-dependent killing curve.

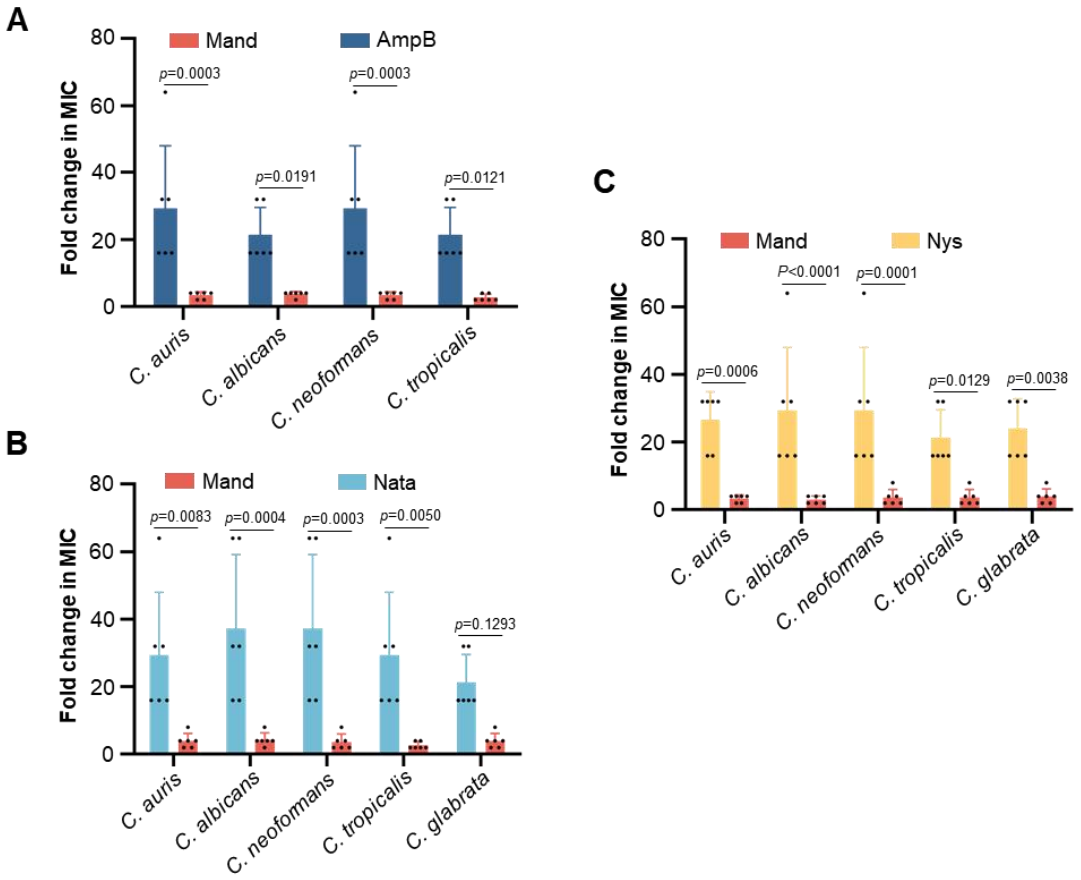

Fig S14. MIC-fold change for mandimycin and amphotericin B against various resistant colonies. (A) Amphotericin B-resistant fungal isolates; (B) Natamycin-resistant fungal isolates; (C) Nystatin-resistant fungal isolates. (Data are presented as mean ± SD, two-way analysis of variance (ANOVA), n = 6 biological replicates).

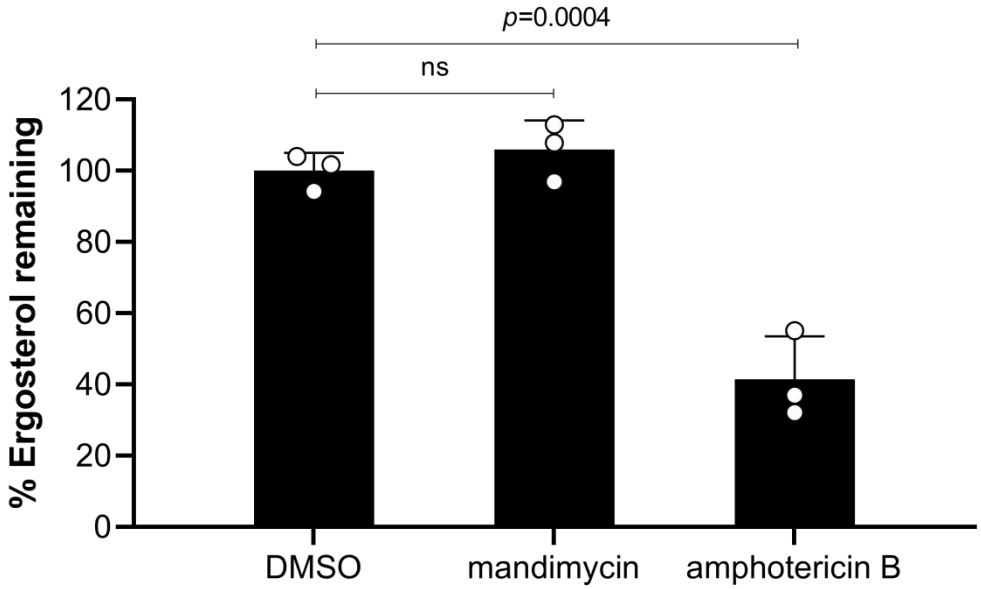

Fig S15. Percent ergosterol remaining in the cell membranes of *C. albicans* BNCC 186382 after treatment with 5 µM mandimycin or 5 µM amphotericin B. The percentage of ergosterol remaining was normalized to values from controls treated with DMSO only. Data are represented as mean ± SD, (n = 3 biological replicates). Significant differences between groups were analyzed using one-way analysis of variance (ANOVA).

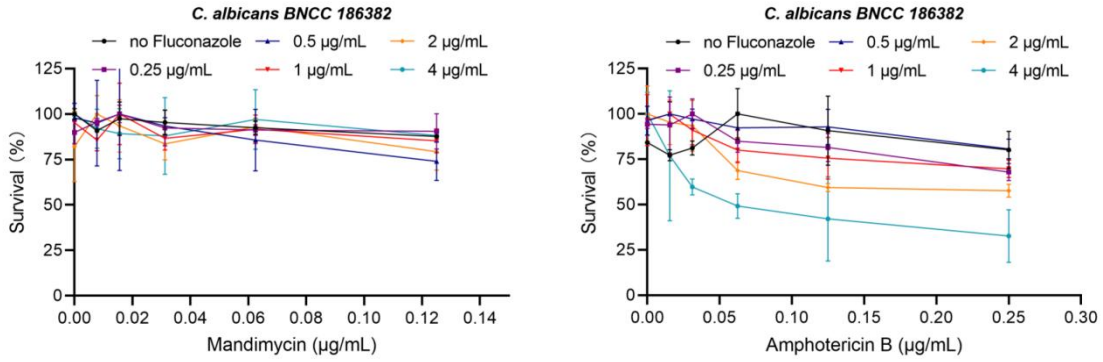

Fig S16. Survival rate of *C. albicans* BNCC 186382 treated with mandimycin or amphotericin B in the presence of varying concentration of the ergosterol biosynthesis inhibitor fluconazole. The OD_{600} of the overnight culture without any antibiotic treatment was normalized as 100% survival, while the OD_{600} of the wells with no bacteria growth was considered as 0% survival. Data are represented as mean ± SD (n = 3 technical replicates).

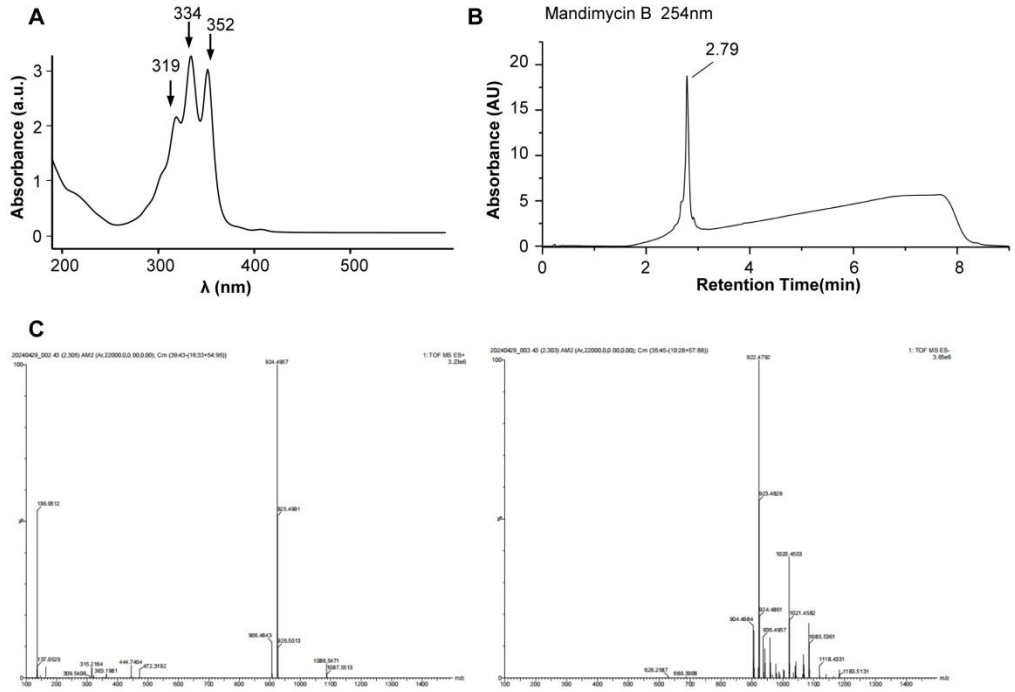

Fig S17. Spectroscopic parameters of mandimycin B. (A) UV-vis spectra of mandimycin B showing the maximum UV adsorptions. (B) HPLC spectrum of purified mandimycin B detected at a wavelength of 254 nm. (C) HR-ESI-MS spectra of mandimycin B under both positive and negative ionization modes.

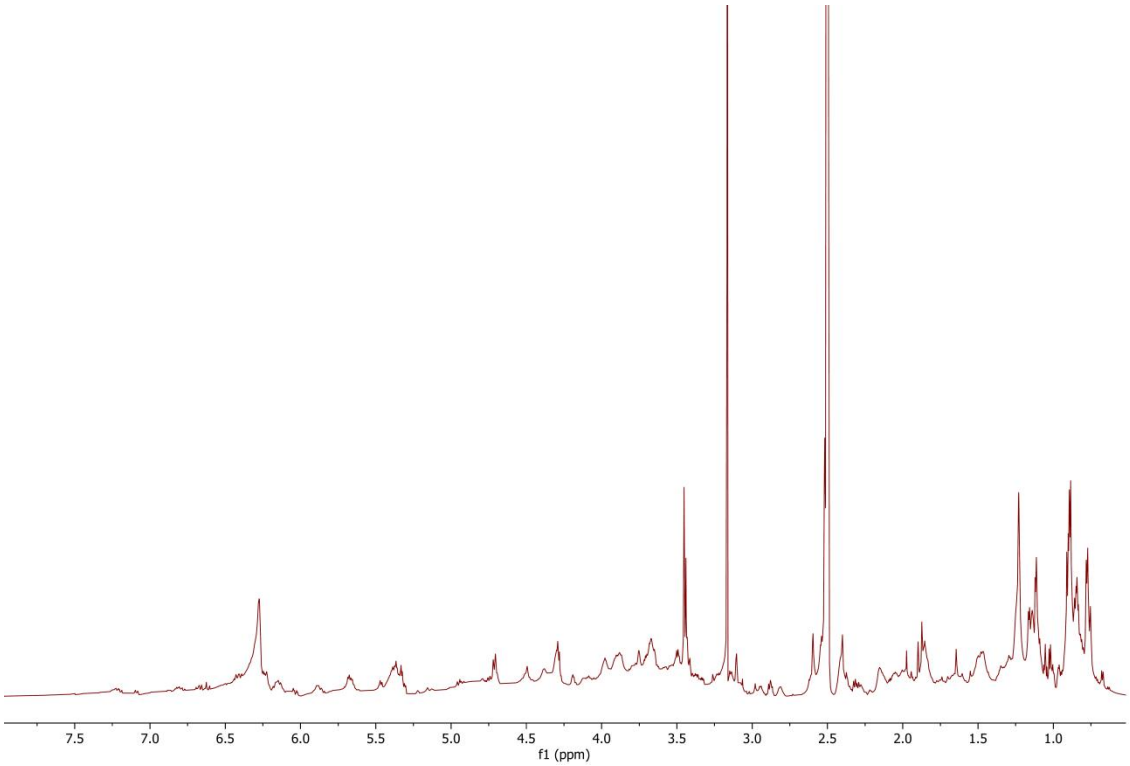

Fig S18. ^{1}H NMR (700 MHz) spectrum of mandimycin B in DMSO-d_6

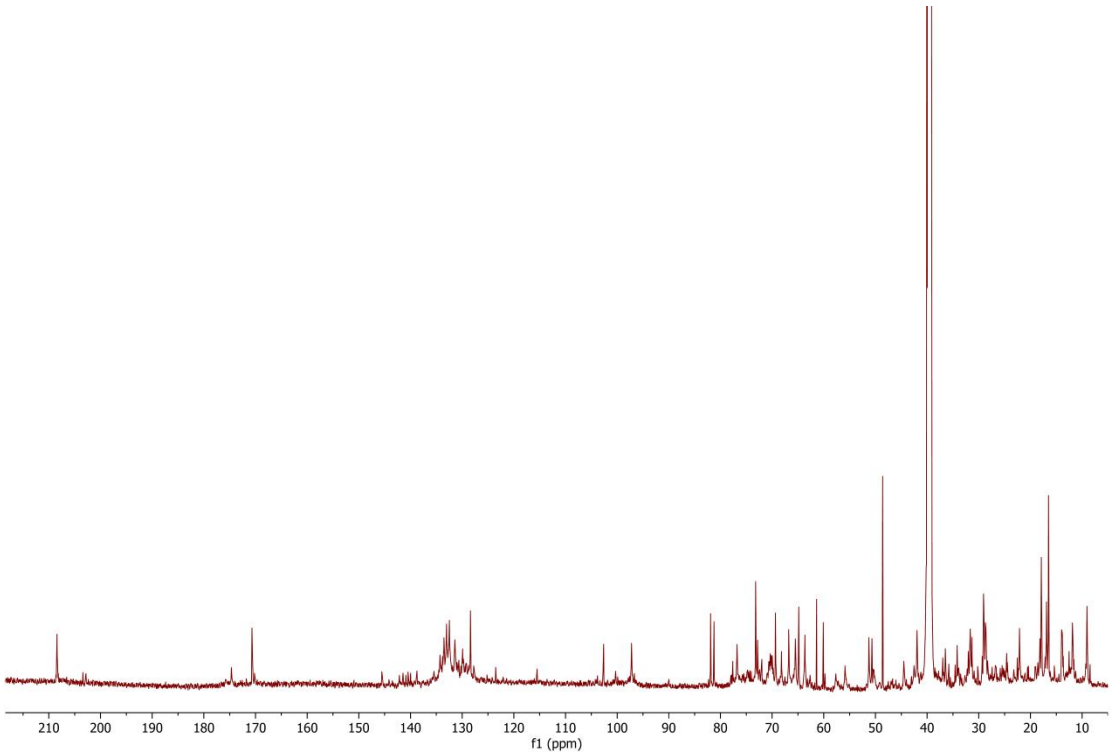

Fig S19. ^{13}C NMR (175 MHz) spectrum of mandimycin B in DMSO-d_6

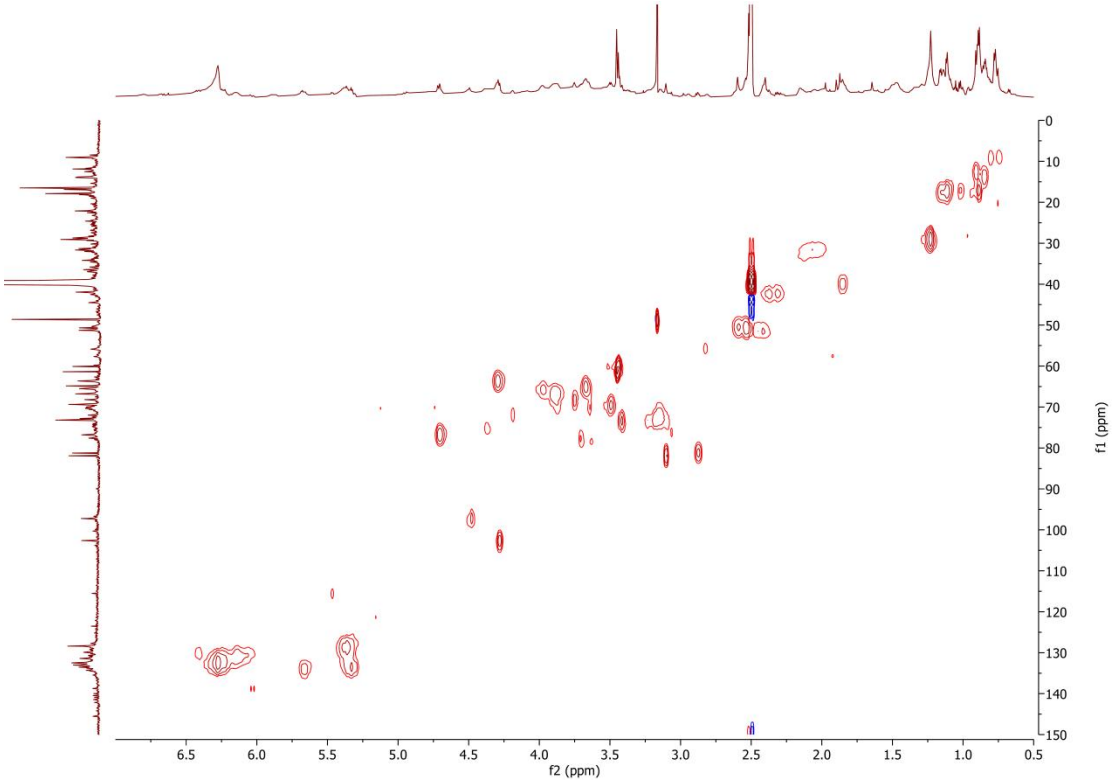

Fig S20. HSQC NMR (175 MHz) spectrum of mandimycin B in DMSO-d_6

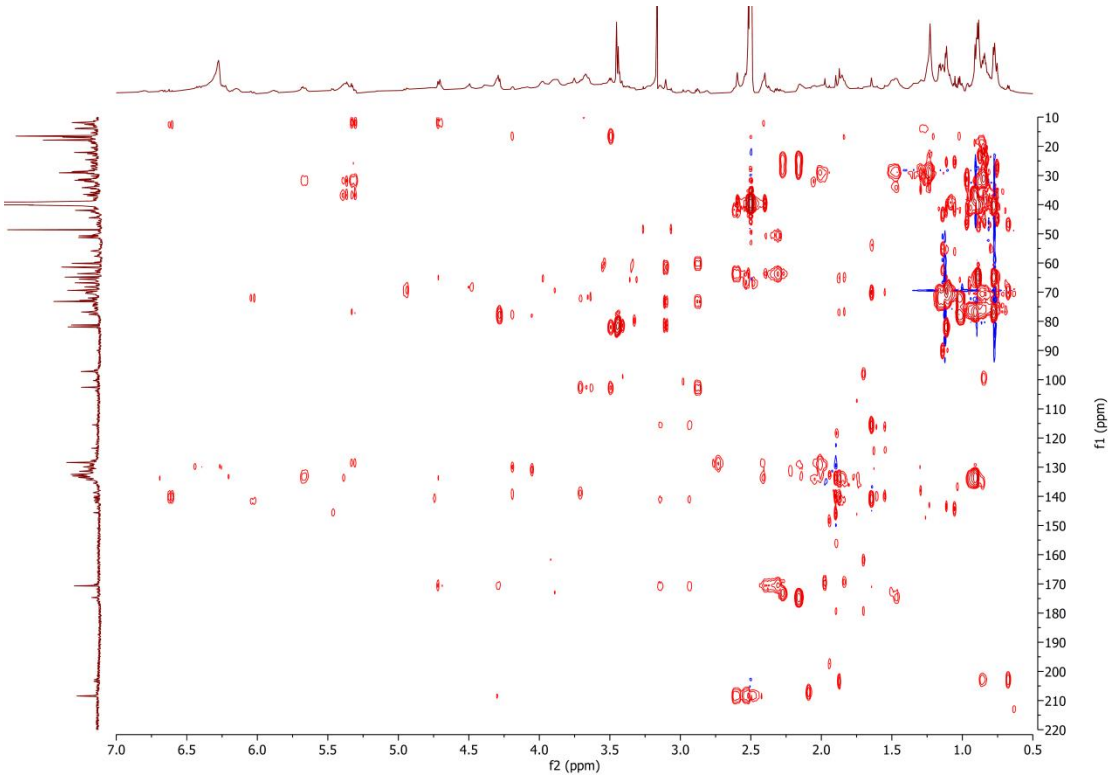

Fig S21. HMBC NMR (175 MHz) spectrum of mandimycin B in DMSO-d_6

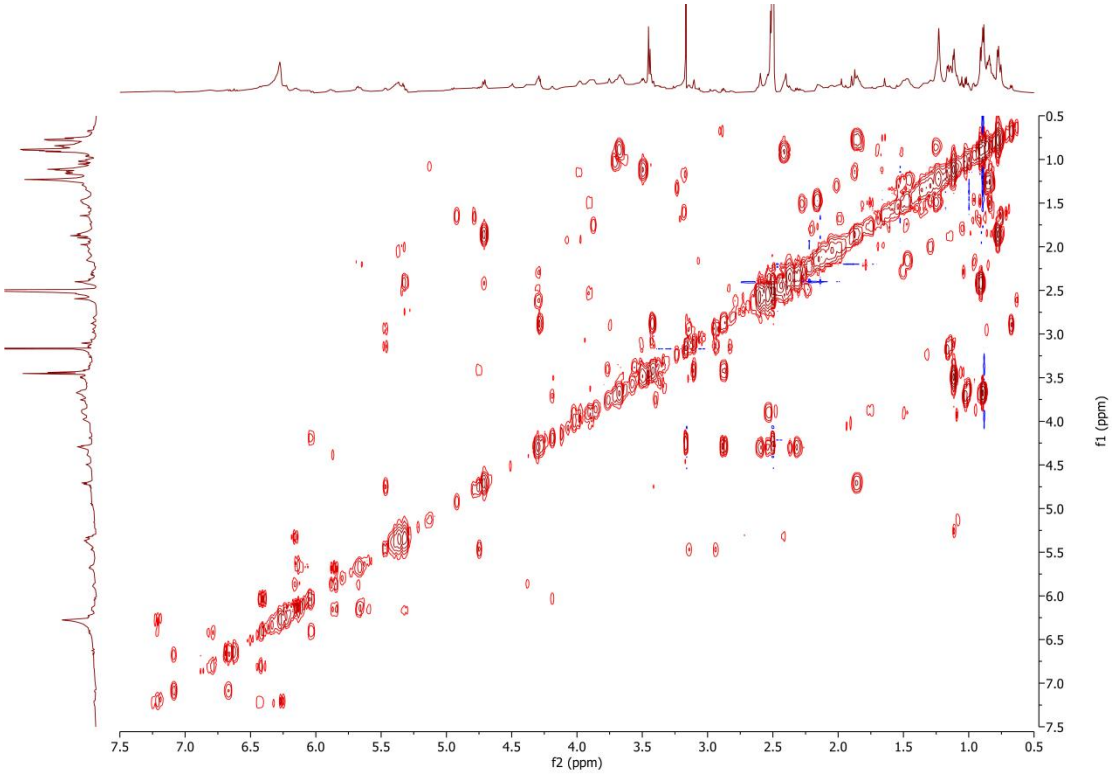

Fig S22. COSY NMR (700 MHz) spectrum of mandimycin B in DMSO-d_6

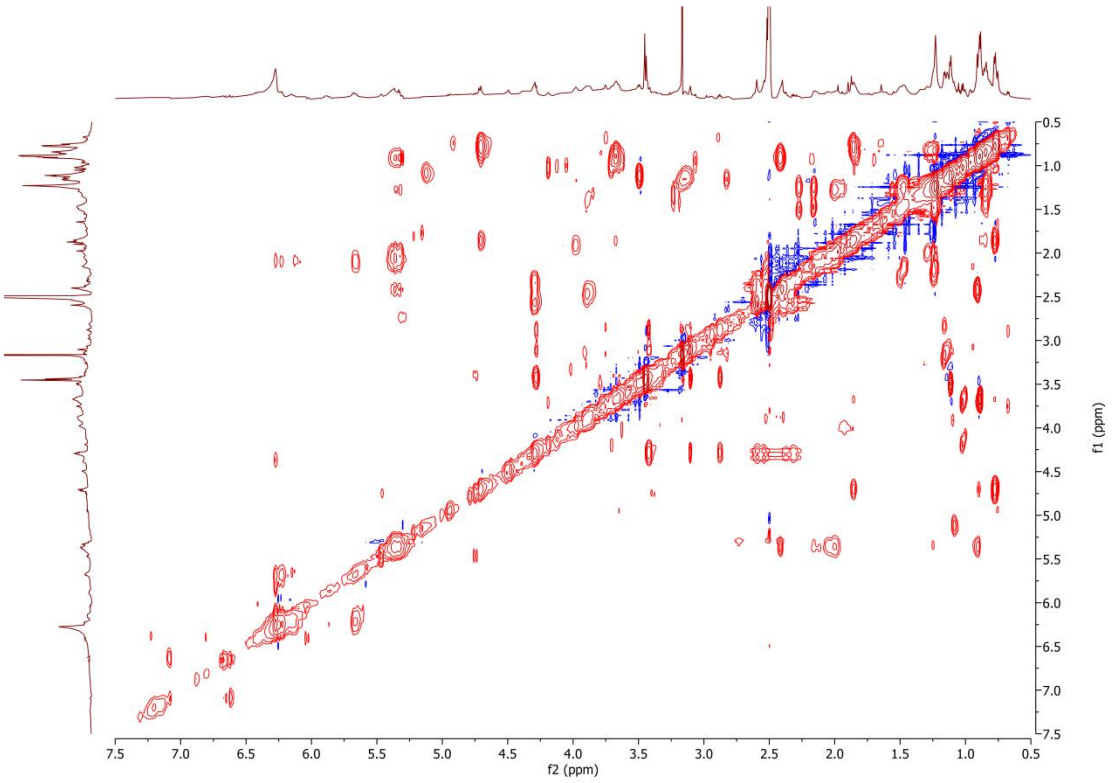

Fig S23. TOCSY NMR (700 MHz) spectrum of mandimycin B in DMSO-d_6

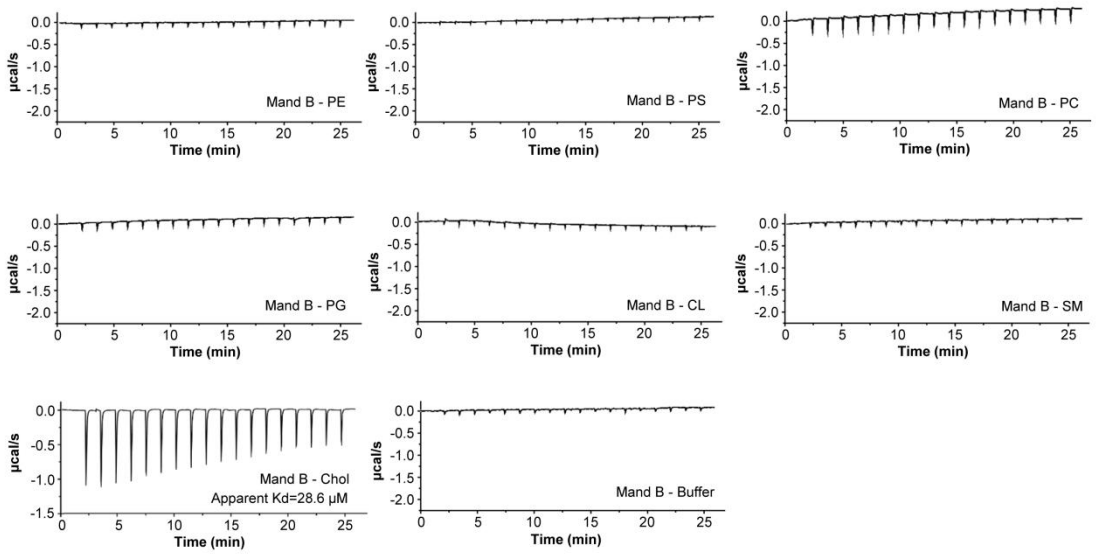

Fig S24. ITC plots of mandimycin B titrated with different fungal cell membrane components

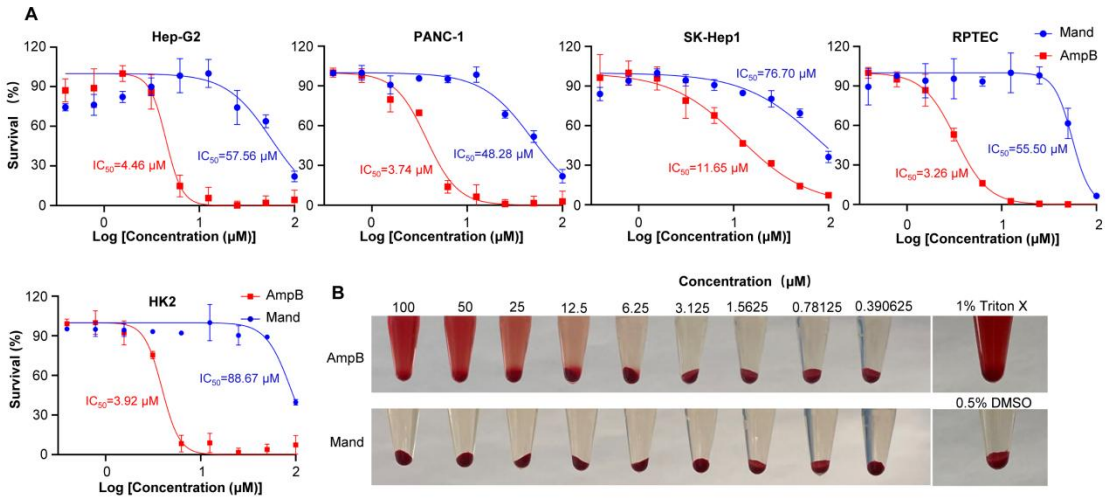

Fig S25. *In vitro* toxicity assay of mandimycin using amphotericin B as the control. (A) Cytotoxicity of mandimycin and amphotericin B against HepG2, PANC-1, SK-Hep1, RPTEC, and HK2 cell lines(n = 3 biological replicates, Data are represented as mean ± SD). (B) Photos of mandimycin and amphotericin B hemolysis assay. .

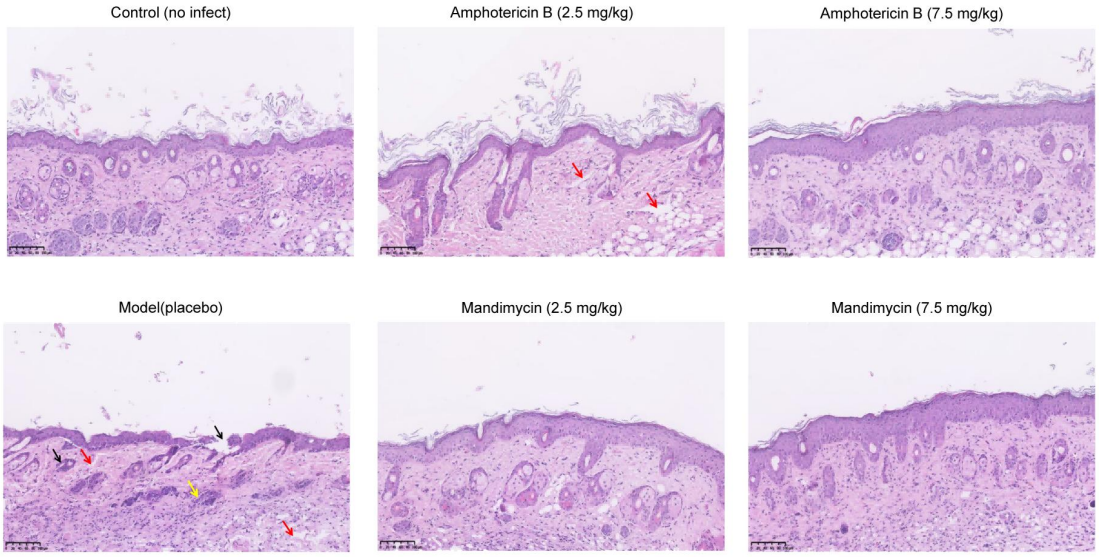

Fig S26. Hematoxylin-eosin (H&E) staining for mouse skin after full-thickness skin perforation and *C. albicans* infection. Black arrow, the loss of sweat glands and hair follicles and the fractures of skin surface; yellow arrow, inflammatory cell infiltration; red arrow, tissue edema.

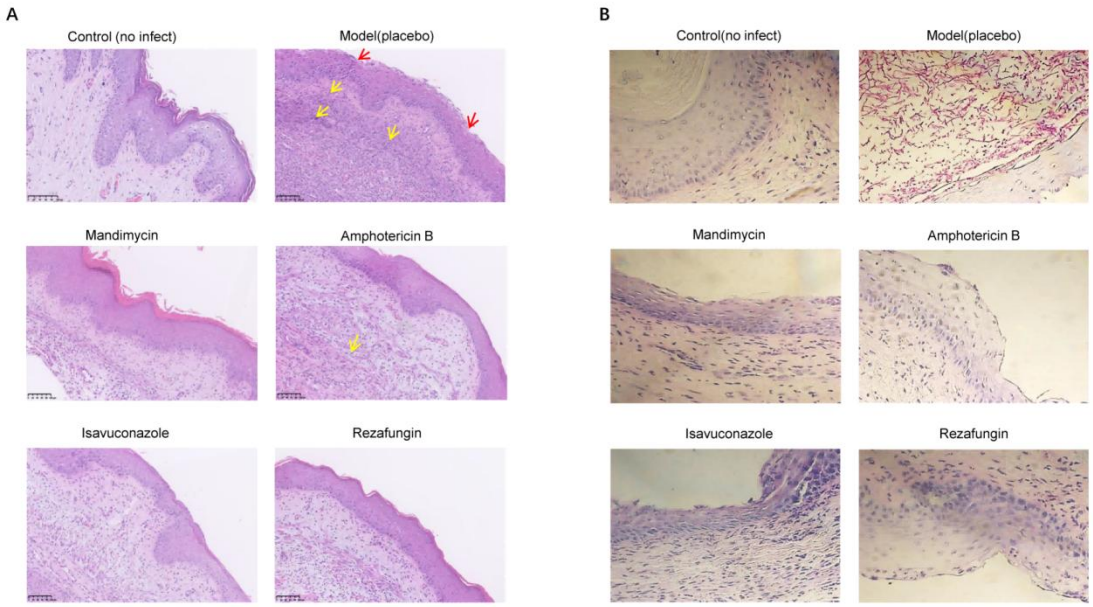

Fig S27. Hematoxylin-eosin (H&E) staining and periodic acid-Schiff (PAS) staining of vaginal sections after *C. albicans* infection. A. Histology of vaginal tissue sections stained with hematoxylin-eosin. Red arrow, damaged vaginal epithelium; yellow arrow, neutrophils infiltrating. B. Representative histological micrographs of PAS staining of vaginal tissue in *C. albicans* on the sixth day after treatment. Magnification, ×400.

Table S1. Characterized glycosyltransferases used in pHMMer model construction

Polyene Macrolide Antibiotic	Glycosyltransferase ID	Protein size(aa)
67-121A	AGM21646.1	457
Amphotericin B	AAK73511.1	483
Candicidin	AAQ82555.1	458
Eurocidin D	WP_102918851.1	459
Lucensomycin	QSE03587.1	474
Natamycin	ADD85130.2	458
NPPA	OLM18863.1	471
NystatinA1	AVX51105.1	463
Pimaricin	CAC20918.1	458
Rimocidin	AAR16517.1	460
Tetramycin	QIZ24108.1	462

Table S2. Mandimycin biosynthetic gene cluster annotation

ORF	Gene name	Size (bp)	Putative Protein, [Source Organism], Accession number	Proposed Function
1	*mandA*	2016	ABC transporter ATP-binding protein/permease [*Streptomyces*]|WP_130880883.1|	Efflux
2	*mandB*	1752	ABC transporter transmembrane domain-containing protein [*Streptomyces syringium*]|WP_245382703.1|	Efflux
3	*mandC*	1032	GDP-mannose 4,6-dehydratase [*Streptomyces* sp. NRRL B-1568]|KJY42921.1|	Mycosamine biosynthesis
4	*mandD*	28422	type I polyketide synthase CP077658.1	PKS modules 9-14
5	*mandE*	16182	type I polyketide synthase [*Streptomyces syringium*]|WP_209518050.1|	PKS modules 15-17
6	*mandF*	6186	type I polyketide synthase [*Streptomyces netropsis*]|WP_130880878.1|	PKS module 18 +thioesterase
7	*mandG*	1188	cytochrome P450 [*Streptomyces*]|WP_130880877.1|	Hydroxylation
8	*mandH*	198	ferredoxin [*Streptomyces*]|WP_242626363.1|	Ferredoxin
9	*mandI*	1176	cytochrome P450 [*Streptomyces*]|WP_130880876.1|	Hydroxylation
10	*mandJ*	1059	DegT/DnrJ/EryC1/StrS family aminotransferase [*Streptomyces*]|WP_130880875.1|	Mycosamine biosynthesis
11	*mandK*	1389	glycosyltransferase [*Streptomyces syringium*]|WP_209518054.1|	Glycosyltransferase
12	*mandL*	3243	type I polyketide synthase [*Streptomyces netropsis*]|WP_229822576.1|	PKS Loading module
13	*mandM*	9492	acyl transferase domain-containing protein/acyl carrier protein [*Streptomyces syringium*]|MBP2406714.1|	PKS modules 1-2
14	*mandN*	32331	type I polyketide synthase [*Streptomyces netropsis*]|	PKS modules 3-8
15	*mandO*	1068	glucose-1-phosphate thymidylyltransferase [*Streptomyces*]|WP_130880348.1|	Digitoxose biosynthesis
16	*mandP*	981	dTDP-glucose 4,6-dehydratase [*Streptomyces netropsis*]|WP_130880349.1|	Digitoxose biosynthesis
17	*mandQ*	1167	glycosyltransferase [*Streptomyces syringium*]|MBP2406718.1|	Glycosyltransferase
18	*mandR*	795	FkbM family methyltransferase [*Streptomyces*]|WP_130880350.1|	4-O-methyl-digitoxose biosynthesis
19	*mandS*	765	NAD-dependent epimerase/dehydratase family protein [*Streptomyces netropsis*]|WP_130880351.1|	Digitoxose biosynthesis
20	*mandT*	576	LuxR family transcriptional regulator [*Streptomyces* sp. NRRL B-1568]|KJY41371.1|	Regulator
21	*mandU*	771	alpha/beta fold hydrolase [*Streptomyces netropsis*]|WP_130880353.1|	Digitoxose biosynthesis

Table S3. ^{1}H and ^{13}C NMR (DMSO-d_6) data for mandimycin

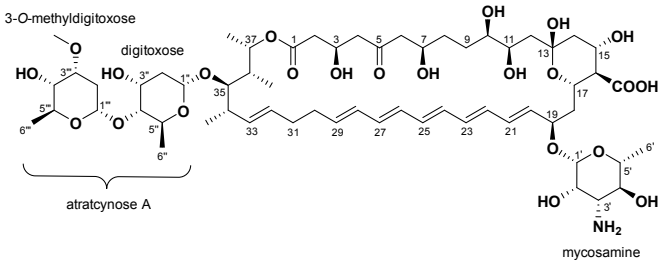

Pos.	δ_C, type*	δ_H, mult. (*J* in	Pos.	δ_C, type*	δ_H, mult. (*J* in
Polyene macrolide			32	129.2, CH	5.37
1	170.1, C		33	133.3, CH	5.34
2	42.3, CH_2	2.27; 2.36	34	38.7, CH	2.34
3	63.7, CH	4.29	35	84.1, CH	3.26
4	50.3, CH_2	2.53; 2.59	36	38.7, CH	1.92
5	208.4, C		37	70.4, CH	5.1
6	51.3, CH_2	2.42; 2.47	16-CO OH	174.8, C	
7	66.9, CH	3.89	34-CH_3	16.7, CH_3	0.93
8	34.2, CH_2	1.33; 1.47	36-CH_3	11.1, CH_3	0.85
9	28.8, CH_2	1.37; 1.49	37-CH_3	15.6, CH_3	1.05
10	66.8, CH	3.91	Mycosamine		
11	65.8, CH	4.00	1′	96.8, CH	4.49
12	44.4, CH_2	1.15; 1.90	2′	67.9, CH	3.79
13	97.2, C		3′	55.7, CH	2.9
14	42.6, CH_2	1.50; 1.71	4′	73.3, CH	3.14
15	65.6, CH	3.98	5′	71.9, CH	3.27
16	57.7, CH	1.94	6′	17.8, CH_3	1.17
17	65.5, CH	4.05	Digitoxose		
18	37.2, CH_2	1.68; 1.86	1″	99.5, CH	4.42
19	74.7, CH	4.36	2″	38.5, CH_2	1.28; 2.08
20	135.1, CH	5.85	3″	68.7, CH	3.45
21	131.2, CH	6.18	4″	86.8, CH	2.96
22	129.1-134.4, CH	6.05-6.32	5″	69.7, CH	3.24
23	129.1-134.4, CH	6.05-6.32	6″	17.8, CH3	1.17
24	129.1-134.4, CH	6.05-6.32	3-*O*-methyldigitoxose		

25	129.1-134.4, CH	6.05-6.32	1‴	100.0, CH	4.61
26	129.1-134.4, CH	6.05-6.32	2‴	35.7, CH2	1.23; 2.30
27	129.1-134.4, CH	6.05-6.32	3‴	79.7, CH	3.14
28	131.4, CH	6.11	4‴	74.7, CH	2.88
29	134.4, CH	5.62	5‴	71.9, CH	3.28
30	31.9, CH_2	2.16	6‴	17.6, CH_3	1.17
31	31.5, CH_2	2.03; 2.15	3‴-OCH_3	56.7, CH_3	3.32

* The assignment of some carbon signals was supported by HSQC and HMBC correlations.

The coupling constants for proton signals were not provided as most signals are highly overlapped or broad.

Table S4. Strains and culture conditions

Cell Type	Organism	Strain/Cell	Media	Culture
Fungal pathogen	*Candida auris*	BNCC 357785	YPD	30℃, aerobic
	Candida auris	BNCC 357784		
	Candida auris	AMR05		
	Candida albicans	BNCC 186382		
	Candida albicans	BNCC 337321		
	Candida albicans	BNCC 336485		
	Cryptococcus neoformans	BNCC 225501		
	Cryptococcus neoformans	BNCC 356067		
	Aspergillus fumigatus	BNCC 122691		
	Aspergillus fumigatus	BNCC 340016		
	Candida glabrata	BNCC 337348		
	Candida tropicalis	BNCC 340288		
	Candida parapsilosis	BNCC 337317		
	Mucor sp.	BNCC 195604		
	Fusarium sp.	BNCC 340967		
	Candida krusei	BNCC 185429		
	Cryptococcus gattii	BNCC 354891		
	Talaromyces marneffei	BNCC 334957		
	Emergomyces pasteurianus	BNCC 362479		
	Exophiala dermatitidis	BNCC 360135		
ESKAPE pathogen	*Enterococcus faecium*	BNCC 186301	LB	37 ℃, aerobic
	Staphylococcus aureus	BNCC 186335		
	Klebsiella pneumoniae	BNCC 186113		
	Acinetobacter baumannii	BNCC 194496		
	Pseudomonas aeruginosa	BNCC 186070		
	Enterobacter cloacae	BNCC 185928		
Fermentation bacteria	*Streptomyces netropsis*	DSM 40259	MS	30 ℃, aerobic
Human cells	HepG2	TCHu72	DMEM +10% FBS	37 ℃, 5% CO_2
	HK2	ATCC-CRL-1469	RPMI-1640	

		+10% FBS
PANC-1	ATCC-CRL-2190	DMEM +10% FBS
SK-Hep1	TCHu109	DMEM +10% FBS
RPTEC	ATCC-PCS-400-010	Renal epithelial cell basal media+renal epithelial growth kit

Table S5. MIC values of mandimycin against a panel of ESKAPE pathogens

Type	Organism	Isolate	MIC (μg/mL)
ESKAPE	*Enterococcus faecium*	BNCC186301	>64
	Staphylococcus aureus	BNCC186335	>64
	Klebsiella pneumoniae	BNCC186113	>64
	Acinetobacter baumannii	BNCC194496	>64
	Pseudomonas aeruginosa	BNCC186070	>64
	Enterobacter cloacae	BNCC185928	>64

Table S6. The number of fungal resistant colonies developed in response to different antifungal agents

Mother strain	**Mutation rate**（1×10^{-9}）											
	amphotericin B			natamycin			nystatin			mandimycin		
Candida auris BNCC 357785	8	4	6	18	11	10	4	1	2	0	0	0
Candida albicans BNCC 186382	5	2	7	2	7	4	21	34	16	0	0	0
Cryptococcus neoformans BNCC 225501	17	8	11	52	31	19	2	6	2	0	0	0
Candida tropicalis BNCC 340288	574	612	514	46	32	43	58	49	60	0	0	0
Candid glabrata BNCC 337348	0	0	0	5	3	6	30	22	19	0	0	0

Table S7. Stoichiometry of mandimycin and phospholipids calculated by the ITC titration assay. The experiments were performed three time independently.

Phospholipids	N values (stoichiometry)				
	Test1	Test2	Test3	Mean value	SD value
PI	0.39	0.40	0.36	0.38	0.021
PE	0.60	0.67	0.62	0.63	0.036
PS	0.51	0.49	0.58	0.53	0.047
PG	0.59	0.55	0.56	0.57	0.021
PC	0.58	0.54	0.50	0.54	0.040
SM	0.61	0.65	0.57	0.61	0.040
CL	0.48	0.53	0.49	0.50	0.026

Table S8. ^{1}H and ^{13}C NMR (DMSO-d_6) data for mandimycin B

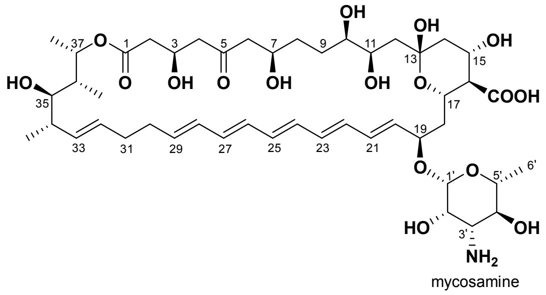

Pos.	δ_C, type*	δ_H, mult. (*J* in Hz)#	Pos.	δ_C, type*	δ_H, mult. (*J* in Hz)#
Polyene macrolide					
1	170.7, C		25	129.9-134.4, CH	6.08-6.28
2	41.8, CH_2	2.30; 2.38	26	129.9-134.4, CH	6.08-6.28
3	63.8, CH	4.30	27	129.9-134.4, CH	6.08-6.28
4	50.7, CH_2	2.53; 2.60	28	130.8, CH	6.13
5	208.4, C		29	134.3, CH	5.66
6	51.3, CH_2	2.43; 2.47	30	32.2, CH_2	2.13
7	66.7, CH	3.92	31	31.3, CH_2	2.02; 2.11
8	33.6, CH_2	1.32; 1.49	32	128.4, CH	5.38
9	28.5, CH_2	1.36; 1.43	33	133.6, CH	5.33
10	66.7, CH	3.89	34	36.8, CH	2.41
11	65.7, CH	3.98	35	76.8, CH	4.71
12	44.5, CH_2	1.15; 1.90	36	40.2, CH	1.85
13	97.2, C		37	64.8, CH	3.67
14	42.7, CH_2	1.49; 1.70	16-COOH	174.7, C	
15	66.0, CH	3.98	34-CH_3	16.9, CH_3	0.91
16	57.6, CH	1.94	36-CH_3	8.9, CH_3	0.77
17	65.8, CH	4.03	37-CH_3	16.9, CH_3	0.89
18	37.4, CH_2	1.65; 1.91	Mycosamine		
19	74.8, CH	4.36	1′	97.3, CH	4.49
20	135.0, CH	5.87	2′	68.2, CH	3.76
21	131.0, CH	6.16	3′	56.0, CH	2.91
22	129.9-134.4, CH	6.08-6.28	4′	73.3, CH	3.14
23	129.9-134.4, CH	6.08-6.28	5′	71.6, CH	3.20
24	129.9-134.4, CH	6.08-6.28	6′	17.9, CH_3	1.16

* The assignment of carbon signals was supported by HSQC and HMBC correlations.

[#] The coupling constants for proton signals were not provided as most signals are highly overlapped or broad.

Table S9. MIC values of mandimycin B against a panel of fungal pathogens

Organism	Strain	MIC (μg/mL)		
		Mandimycin	Mandimycin B	Amphotericin B
Candida auris	BNCC 357785	1	2	1
Candida albicans	BNCC 186382	0.25	1	0.5
Cryptococcus neoformans	BNCC 225501	0.125	0.5	0.0625
Aspergillus fumigatus	BNCC 122691	2	2	1
Candida krusei	BNCC 185429	2	4	1
Mucor sp.	BNCC 195604	0.25	0.5	0.125
Fusarium sp.	BNCC 340967	1	1	1

References:

1 Van Arnam, E. B. et al. Selvamicin, an atypical antifungal polyene from two alternative genomic contexts. *Proc. Natl. Acad. Sci. USA* **113**, 12940-12945 (2016).

2 Tevyashova, A. N. et al. Semisynthetic Amides of Polyene Antibiotic Natamycin. *ACS Infect. Dis.* **9**, 42-55 (2023).

3 Volpon, L. & Lancelin, J. M. Solution NMR structure of five representative glycosylated polyene macrolide antibiotics with a sterol-dependent antifungal activity. *Eur. J Biochem.* **269**, 4533-4541 (2002).

4 Wu, K. J. Y. et al. An antibiotic preorganized for ribosomal binding overcomes antimicrobial resistance. *Science* **383**, 721-726 (2024).

5 Davis, S. A. et al. Nontoxic antimicrobials that evade drug resistance. *Nat. Chem. Biol.* **11**, 481-487 (2015).

6 Heleno, S. A. et al. Optimization of microwave-assisted extraction of ergosterol from Agaricus bisporus L. by-products using response surface methodology. *Food Bioprod. Process.* **100**, 25-35 (2016).